PROCEEDINGS, 44th Workshop on Geothermal Reservoir Engineering
Stanford University, Stanford, California, February 11-13, 2019
SGP-TR-214

Real-Time Microearthquake Event Detection and Location Using a Multiscale Scanning Approach for EGS Collab Experiments

Yu Chen[1], Lianjie Huang[1], Martin Schoenball[2], Jonathan Ajo-Franklin[2], Timothy J. Kneafsey[2], and EGS Collab Team[*]

[1]Los Alamos National Laboratory, Los Alamos, NM 87545, USA

[2]Lawrence Berkeley National Laboratory, Berkeley, CA 94720, USA

chenyu@lanl.gov; ljh@lanl.gov

Keywords: Correlation coefficient, Enhanced Geothermal Systems, EGS Collab, EGS stimulation, MEQ detection, MEQ location, microearthquake, multiscale, real-time, STA/LTA

ABSTRACT

The U.S. is conducting collaborative research under the EGS Collab project supported by the U.S. Department of Energy's Geothermal Technologies Office to understand the fracture creation and imaging during fracturing in enhanced geothermal systems. Real-time, automatic microearthquake detection and location provides useful information on fracture growth during stimulation. We study the capability of our newly developed multiscale event scanning method for real-time microearthquake monitoring using microearthquake data acquired during the EGS Collab Experiment I. We compute correlation coefficients between STA/LTA (short-time average/long-time average) of recorded seismograms and those of pre-calculated microearthquake waveforms in a database using a moving time window, and search for the grid points with the highest correlation coefficients to detect and locate microearthquake events simultaneously. Our multiscale event scanning method requires much less computation cost than that of the global search for all grid points and every scanning time step, making real-time microearthquake detection and location feasible. We apply our method to microearthquake data acquired during the EGS Collab Experiment I. Compared to LBNL's high-precision location results for 676 events, our method detects approximately 90% of those events with correlation coefficients greater than 0.6 and a standard deviation difference smaller than 2 m. We detect 827 MEQs and 6286 MEQs with correlation coefficients greater than 0.7 and 0.6, respectively. Our real-time MEQ detection and location results reveal the stimulation-created and possible pre-existing fractures. The average computational cost for detecting and locating one event is approximately one second. Our results demonstrate that our newly developed multiscale scanning method is capable of reliably detecting and locating MEQs in nearly real time during EGS stimulations.

1. INTRODUCTION

Under the EGS Collab project supported by the U.S. Department of Energy's Geothermal Technologies Office (GTO), U.S. national laboratories, universities and industrial collaborations are conducting intermediate-scale (on the order of 10 m) field experiments to refine our understanding of rock mass response to stimulation. The project provides a test bed for the validation of thermal hydrological-mechanical-chemical (THMC) modeling approaches as well as novel monitoring tools (Dobson et al., 2017; Kneafsey et al., 2018).

Real-time microearthquake (MEQ) monitoring is currently the most efficient approach to obtaining a spatio-temporal image of fracture growth during stimulation. Real-time monitoring is a standard operational procedure for a traffic-light stimulation system attempting to control injection and mitigate risk of induced earthquakes (Maxwell, 2014). During stimulation experiments, it is important to identify the direction and extension of fracture growth, and understand the relationship between injection rates and fracture growth during stimulation. EGS stimulation could also trigger geohazards on pre-existing faults or cause a rupture in an unexpected direction, which requires real-time monitoring.

Various MEQ detection and location methods have been developed for real-time monitoring. We classify previous studies into three categories. The first category of the methods detects seismic phases and invert arrival-times of those seismic phases (e.g. Khadhraoui et al., 2010). These methods are the least time consuming. However, it is difficult to distinguish seismic phases, particularly for MEQ data with very unclear first arrival phases. The second category of the methods is based on cross-correlation of MEQ waveforms between recorded and template waveforms (e.g. Zhang and Zhang, 2016). It is challenging to obtain template waveforms for real-time detection.

---

[*] J. Ajo-Franklin, S.J. Bauer, T. Baumgartner, K. Beckers, D. Blankenship, A. Bonneville, L. Boyd, S.T. Brown, J.A. Burghardt, T. Chen, Y. Chen, K. Condon, P.J. Cook, P.F. Dobson, T. Doe, C.A. Doughty, D. Elsworth, J. Feldman, A. Foris, L.P. Frash, Z. Frone, P. Fu, K. Gao, A. Ghassemi, H. Gudmundsdottir, Y. Guglielmi, G. Guthrie, B. Haimson, A. Hawkins, J. Heise, C.G. Herrick, M. Horn, R.N. Horne, J. Horner, M. Hu, H. Huang, L. Huang, K. Im, M. Ingraham, T.C. Johnson, B. Johnston, S. Karra, K. Kim, D.K. King, T. Kneafsey, H. Knox, J. Knox, D. Kumar, K. Kutun, M. Lee, K. Li, R. Lopez, M. Maceira, N. Makedonska, C. Marone, E. Mattson, M.W. McClure, J. McLennan, T. McLing, R.J. Mellors, E. Metcalfe, J. Miskimins, J.P. Morris, S. Nakagawa, G. Neupane, G. Newman, A. Nieto, C.M. Oldenburg, W. Pan, R. Pawar, P. Petrov, B. Pietzyk, R. Podgorney, Y. Polsky, S. Porse, S. Richard, B.Q. Roberts, M. Robertson, W. Roggenthen, J. Rutqvist, D. Rynders, H. Santos-Villalobos, M. Schoenball, P. Schwering, V. Sesetty, A. Singh, M.M. Smith, H. Sone, C.E. Strickland, J. Su, C. Ulrich, N. Uzunlar, A. Vachaparampil, C.A. Valladao, W. Vandermeer, G. Vandine, D. Vardiman, V.R. Vermeul, J.L. Wagoner, H.F. Wang, J. Weers, J. White, M.D. White, P. Winterfeld, T. Wood, H. Wu, Y.S. Wu, Y. Wu, Y. Zhang, Y.Q. Zhang, J. Zhou, Q. Zhou, M.D. Zoback

The third category of the methods migrates seismic energy back to the best hypocenter location (e.g., Nakata and Beroza, 2016). These methods have potential to search MEQs in real time. However, it is also difficult to distinguish seismic phases used in these methods.

In our previous study, we developed a multiscale event scanning approach for real-time detection and location of MEQ events using seismic waveform envelope fitting (Chen et al., 2018b). Our method first uses an elastic-wave modeling tool to pre-compute an MEQ waveform database. We then scan the largest correlation coefficients of envelopes among moving time windows between the recorded seismograms and the waveform database seismograms to detect and locate MEQ events simultaneously. We find that the method is not very robust for applying to field MEQ data containing significant noise.

We improve our multiscale scanning approach for real-time MEQ detection and location using correlation between STA/LTA (ration of short-time average and long-time average) of MEQ data and that of synthetic MEQ data. The new method is more robust for noisy MEQ data. We apply our new method to MEQ data acquired during the Experiment I of the EGS Collab project. We compare our results for some selected events with those obtained using a standard location method employed by Schoenball et al., (2019). We apply our method to MEQ data acquired from May to July, 2018, and detect 827 MEQs and 6286 MEQs with correlation coefficients greater than 0.7 and 0.6, respectively. The standard deviation difference between our and their MEQ locations is less than 2 m. Our real-time MEQ detection and location results reveal not only the stimulation-created fractures, but also possible pre-existing fractures. The average computational cost for detecting and locating one event is approximately one second using 12 cores on a desktop workstation with a 2.3 GHz Xeon processor. Our results demonstrate that our newly developed multiscale scanning method is capable of reliably detecting and locating MEQs in nearly real time during EGS stimulations.

2. SEISMIC MONITORING ARRAY

The EGS Collab project initiated a field experiment at the Sanford Underground Research Facility (SURF) site located at the former site of the Homestake Gold Mine in Lead, South Dakota, in 2018. The experiment is located within a drift, approximately 1.5 km beneath the surface. The microseismic monitoring array is designed to detect MEQs and monitor fracture growth. Six monitoring wells were drilled before stimulation in 2018, as shown in yellow cylinders in Figure 1. Four of these wells (PST, PSB, PDT and PBT in Figure 1) are parallel to the potential stimulation-created fractures, and two wells (OT, OB in Figure 1) are orthogonal to the created fractures. Twelve 3C accelerometers (PCB 356B18), illustrated by black spheres in Figure 1, are deployed within the monitoring wells. An injection well (green cylinder in Figure 1) and a production well (red cylinder in Figure 1) were drilled to create multiple fractures (green circles in Figure 1) with the diameters of approximately 10 m (Kneafsey et al., 2018). MEQ data are recorded on a high-performance 64 channel digitizer (Data Translation VibBox) sampling sensors at 100 kHz. The MEQ seismograms are filtered using a bandpass filter from 5 kHz to 40 kHz.

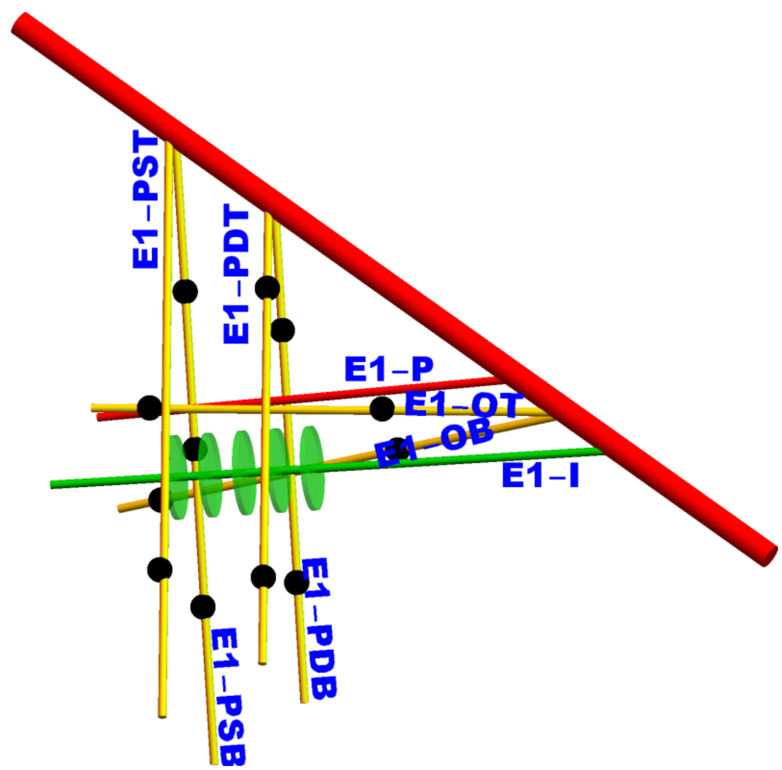

Figure 1: Schematic illustration of the monitoring accelerometers at SURF for the EGS Collab Experiment 1. The monitoring wells drilled from the drift (red cylinder) are in yellow. The injection well is in green, and the production well is in red. The circular regions in green are the fractures to be created by EGS stimulations. The geophones (black spheres) are distributed within the monitoring wells in yellow to monitor induced MEQs evenly distributed within the created fractures in the green circular regions.

3. METHODOLOGY

We recently developed a multiscale scanning approach for real-time detection and location of MEQ events using seismic waveform envelope fitting (Chen et al., 2018b). The method consisted of three steps. When the STA/LTA value is higher than a threshold, the multiscale event scanning is triggered to search a MEQ location to match STA/LTA of the recorded data. The multiscale event scanning algorithm is used for grid-search to obtain the best occurring time and hypocenter location using the highest correlation coefficients between waveform envelopes of the recorded data and the synthetics in 3D space.

We schematically illustrate the multiscale scanning method in 2D in Figure 2. To determine the grid points with the largest correlation coefficients, we first compute correlation coefficients of waveform envelopes within a coarse grid, such as a 7 x 7 x 7 grid (Scale 1 grid on the left panel of Figure 2). For the EGS Collab experiment, we use a grid interval of 6 m for the coarse grid. The time step for moving time windows to calculate correlation coefficients is 20 time sample intervals of MEQ waveforms. After scanning Scale 1 grids (the left panel in Figure 2) and obtaining a grid point with one of the highest correlation coefficients, we continue to scan within a finer grid Scale 2 grid on the right panel of Figure 3), such as a 7 x 7 x 7 grid with a grid interval of 1 m centered on the inverted grid point on the Scale 1 grid, and determine a grid point with the largest correlation coefficient of MEQ waveforms. During the scanning process in Scale 2, the time step for the moving windows to calculate the correlation coefficients is one sample interval of MEQ waveforms. We can continue to scan grid points within a finer grid, till achieving the spatial resolution needed for real-time monitoring. We use a 1-m grid as the finest grid in this study.

When applying our previously developed multiscale scanning method based on waveform envelope correlation to MEQ data from the EGS Collab project, we find that the method is not very robust for noisy data.

We improve our multiscale scanning approach for real-time MEQ detection and location using correlation between STA/LTA (ration of short-time average and long-time average) of MEQ data and that of synthetic MEQ data, rather than using correlation between waveform envelopes of real and synthetic data. The STA/LTA transformation provides clear onsets for the P and/or S arrivals and suppress the effect of strong noise, but the shapes of waveform envelopes can be severely affected by noise. We use the improved multiscale scanning method to analyze MEQ data acquired in the EGS Collab project.

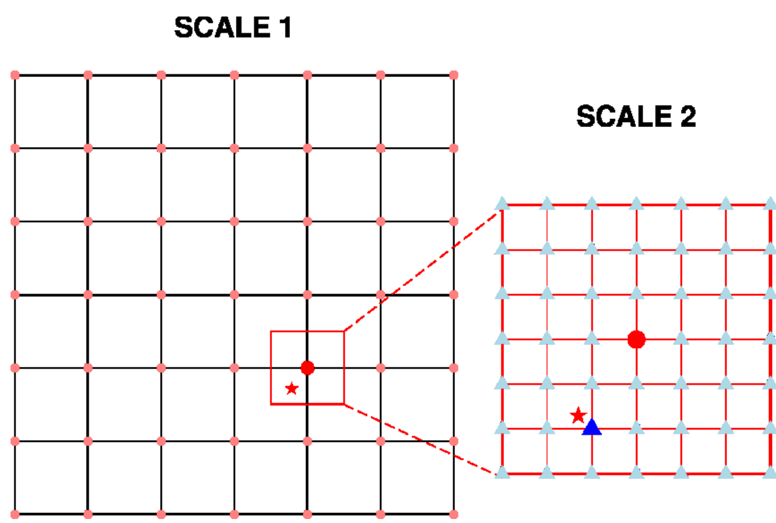

Figure 2: Schematic illustration of our multiscale MEQ event scanning method. Left panel: The heavy red dot represents the inverted MEQ event location in Scale 1 for the true MEQ event labeled as the red star. The red box is the scanning region for Scale 2 with a finer grid. It is centered on the red dot. Right panel: A finer grid (Scale 2) within the red box on the Left panel. The blue triangle represents the inverted MEQ location in Scale 2.

4. VALIDATION USING LBNL'S HIGH-PRECISION MEQ LOCATIONS

To validate the accuracy of our new multiscale scanning method for real-time event detection and location, we compare our event location results with LBNL's high-precision event location results for some selected events that occurred during the EGS Collab Experiment I. LBNL first uses a standard STA/LTA triggering algorithm to detect events, and uses an AIC automatic picker to determine P-phase arrivals and locates MEQs. The locations are further refined using manual arrival-time picks and double-difference relocation. The method uses velocity models, with a P wave velocity of 5.9 km/s and an S wave velocity of 3.3 km/s (Schoenball et al., 2019). They detect 676 MEQs with location uncertainties smaller than 2 m during May to July 2018 for the EGS Collab Experiment I (Figure 3). Blue spheres represent MEQs occurring in May, yellow in June and red in July. The blue and yellow spheres spread out approximately 10 m to the east from the notch at 164 ft, and the red spheres extend approximately 5 - 10 m to the west from the notch at 128 ft.

We apply our real-time multiscale scanning method to the same MEQ data as those used by Schoenball et al. (2019). Among the 676 MEQ events, we detect 596 MEQ events with correlation coefficients greater than 0.6 (Figure 4), or 90% of the events. The remaining events have smaller correlation coefficients. The standard deviation difference between LANL's and LBNL's location results are smaller than 2 m. The MEQ spatial and temporal patterns are consistent between LANL's (Figure 4) and the LBNL's (Figure 3) locations. Both LANL's and LBNL's MEQ location results in May (blue) and June (yellow) in 2018 indicate a hydraulic fracture extended from the notch at 164 ft. Our results show that the fracture is perpendicular to the injection well, while LBNL's results display that the fracture is not exactly perpendicular to the injection well but is slightly tilted. LBNL's location results for MEQs in July (red) in 2018 exhibit a fracture near the notch at 128 ft. Our MEQ locations are closer to the notch at 128 ft, but more scattering. Overall, the MEQ location results obtained using our new multiscale scanning method are generally consistent with LBNL's high-precision location results.

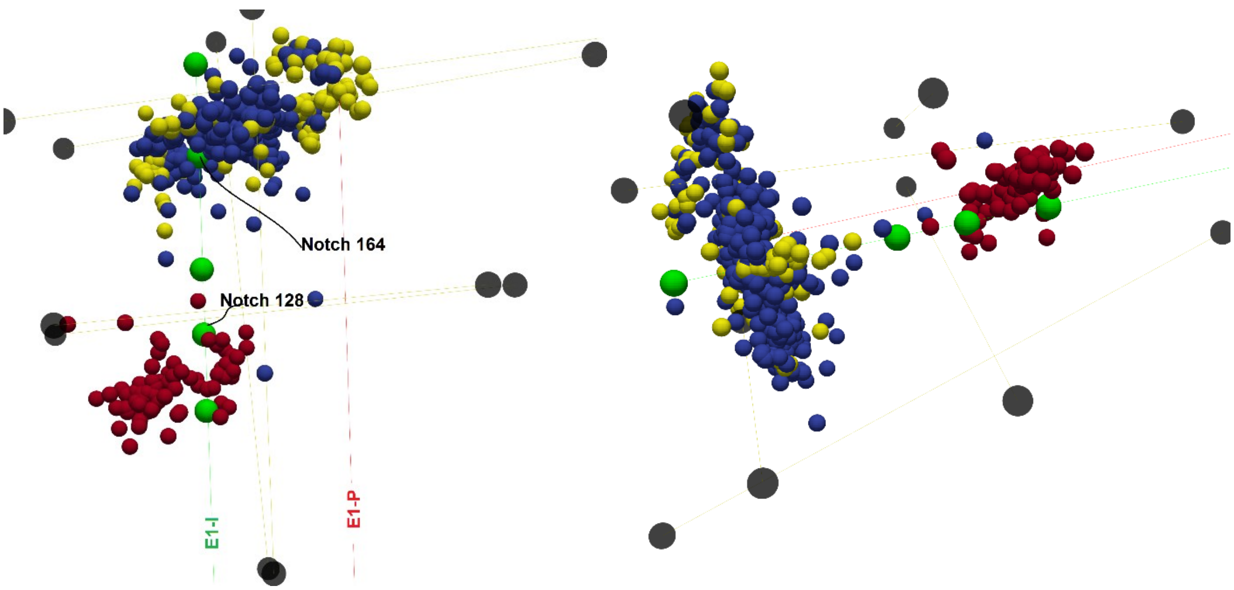

(a) View from the Top (b) View from the West

Figure 3: LBNL's high-precision MEQ locations. Blue spheres represent MEQs occurred in May, yellow for those in June and red for those in July, 2018. Larger black spheres denote the monitoring accelerometers, and green spheres are the stimulation notches.

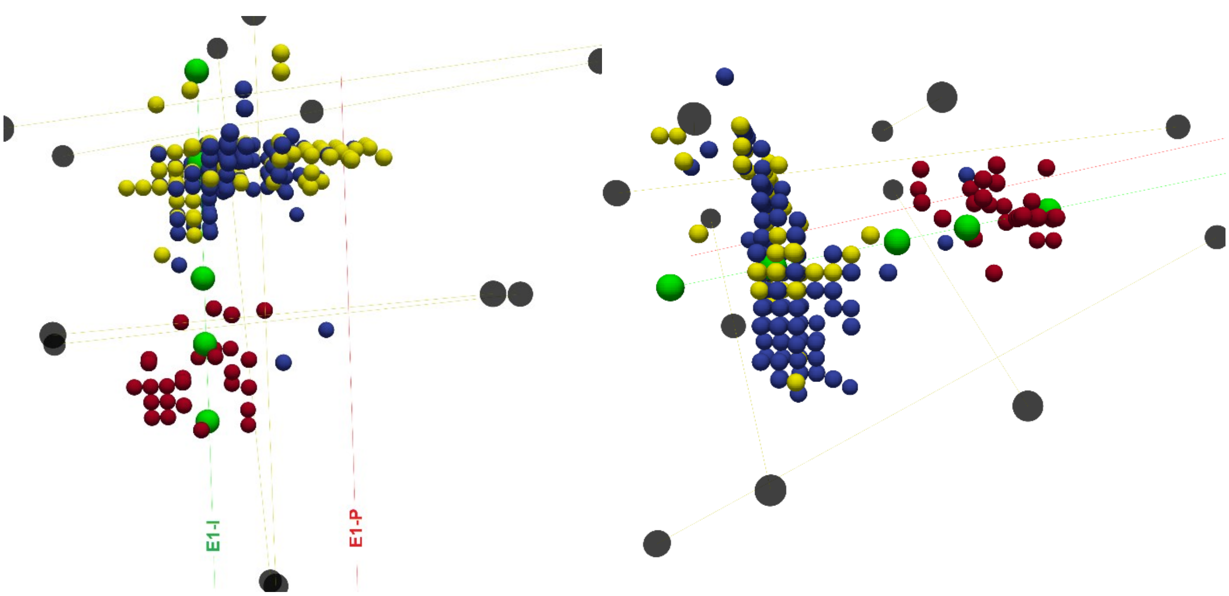

(a) View from the Top (b) View from the West

Figure 4: LANL's MEQ locations for the same MEQ data used for LBNL's high-precision location. Blue spheres represent MEQs occurred in May, yellow for those in June and red for those in July, 2018. Larger black spheres denote the monitoring accelerometers, and green spheres are the stimulation notches.

5. REAL-TIME DETECTION AND LOCATION OF MEQ DATA FROM THE EGS COLLAB EXPERIMENT I

We then apply our new multiscale scanning method to all MEQ data recorded from May to July, 2018 during the EGS Collab Experiment I, and detect and locate 827 and 5459 MEQs with correlation coefficients of STA/LTA greater than 0.7 (Figure 5) and between 0.6 and 0.7 (Figure 6), respectively. Figure 5 reveals similar spatial and temporal patterns to Figure 4, consisting of two hydraulic fractures perpendicular to the injection well at the notch at 164 ft and the notch at 128 ft, respectively. In addition, Figure 5 shows another two fractures parallel to the injection well, which may be pre-existing fractures. One of these two fractures along blue spheres is parallel to the injection well and located on the east side of the well. For MEQs with correlation coefficients between 0.6 and 0.7, Figure 6 shows the same spatial and temporal patterns as those in Figure 5 but more scattering.

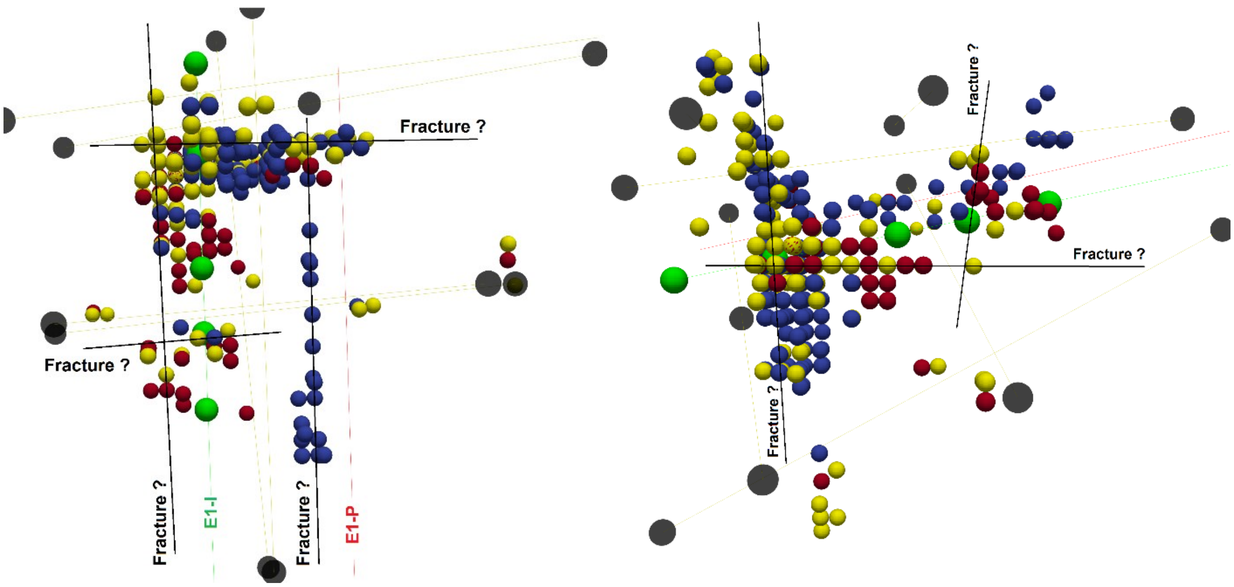

(a) View from the Top (b) View from the West

Figure 5: LANL's MEQ locations with correlation coefficients of STA/LTA greater than 0.7 obtained using our multiscale scanning method. Blue spheres represent MEQs occurred in May, yellow for those in June and red for those in July, 2018. Larger black spheres denote the monitoring accelerometers, and green spheres are the stimulation notches.

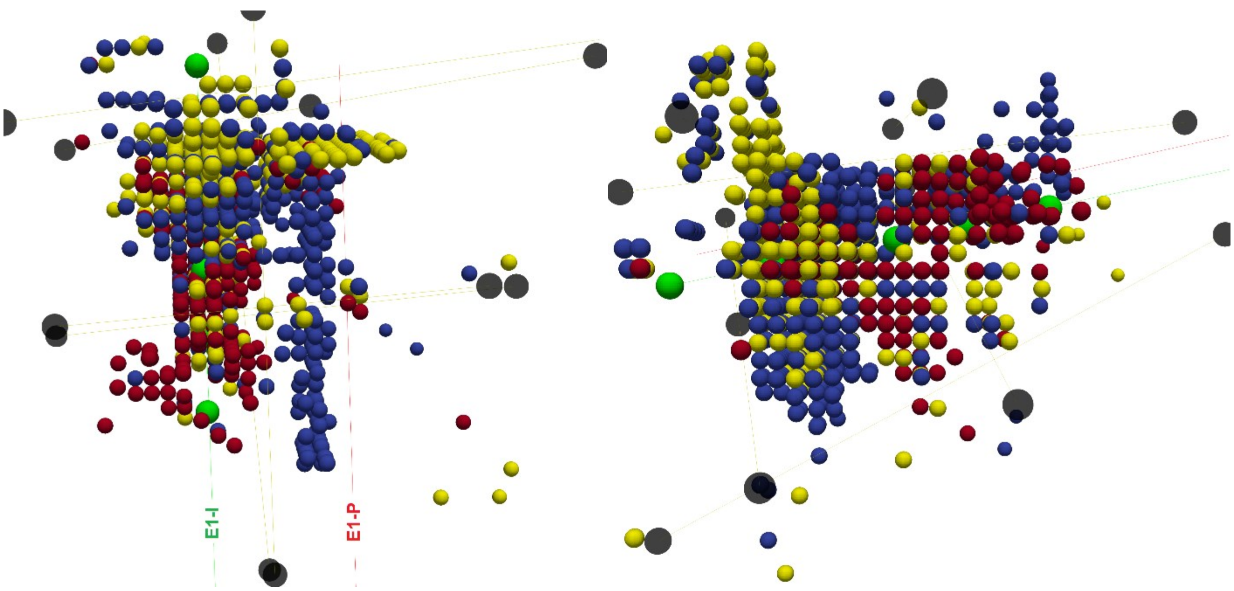

(a) View from the Top (b) View from the West

Figure 6: LANL's MEQ locations with correlation coefficients of STA/LTA between 0.6 and 0.7 obtained using our multiscale scanning method. Blue spheres represent MEQs occurred in May, yellow for those in June and red for those in July, 2018. Larger black spheres denote the monitoring accelerometers, and green spheres are the stimulation notches.

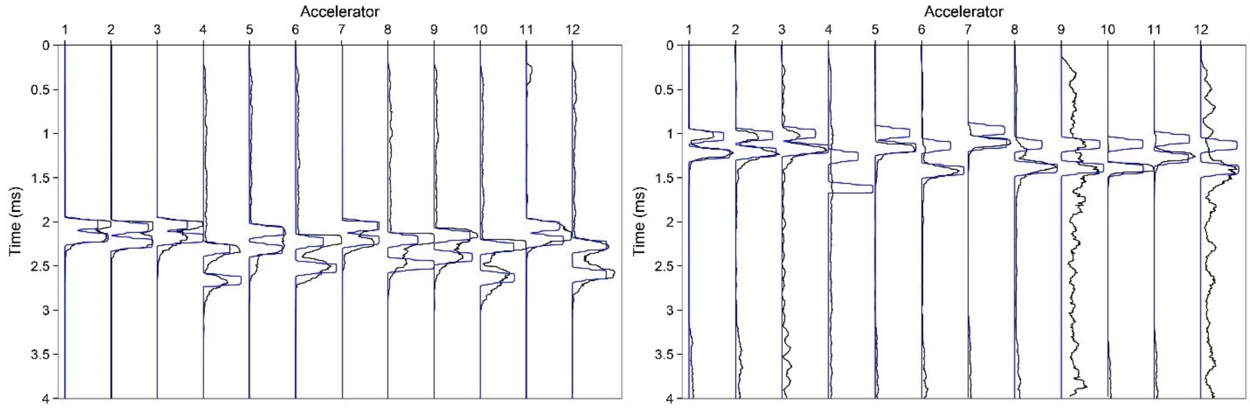

(a) STA/LTA correlation coefficient of 0.83 **(b) STA/LTA correlation coefficient of 0.60**

Figure 7: Examples of STA/LTA fitting with correlation coefficients of 0.83 (a) and 0.60 (b). Black traces in the panels represent the STA/LTA of the recorded MEQ data, and blue traces are the STA/LTA of synthetics.

We show two examples of STA/LTA fitting with correlation coefficients of 0.83 (highest) (Figure 7a) and 0.60 (lowest used) (Figure 7b), respectively. The STA/LTA fittings indicate that our multiscale scanning method can fit the P- and S-phases reasonably well. STA/LTA transformation can greatly reduce seismic noise effect.

We estimate the computation cost to evaluate the capability of real-time detection and location of our method. Our method takes approximately one second of CPU time using 12 cores on a desktop workstation with a 2.3 GHz Xeon processor to detect and locate one event after data are loaded onto the computer.

6. CONCLUSIONS

We have developed a new multiscale scanning method for real-time MEQ monitoring during EGS stimulation. Our new method searches for the event occurring time and hypocenter location using highest correlation coefficients of STA/LTA between recorded MEQ seismograms and a pre-computed MEQ waveform database. The method employs a multiscale event scanning method to greatly reduce the computation cost of the global search for all grid points.

We have validated our method using LBNL's high-precision location results of 676 MEQs occurred during the EGS Collab Experiment I. The standard deviation difference between LANL's and LBNL's location results is smaller than 2 m. The two results display generally consistent spatio-temporal patterns of the MEQs.

We have applied our new multiscale scanning method to all MEQ data recorded during the EGS Collab Experiment I in May to July, 2018, and detected and located 827 MEQs and 6286 MEQs with correlation coefficients greater than 0.7 and 0.6, respectively. Our results show two stimulation-created fractures and two possible pre-existing fractures. The created fractures are perpendicular to the injection well, and the pre-existing fractures are nearly parallel to the well. Our method takes approximately one second of CPU time to detect and locate one MEQ event using 12 cores on a desktop computer with a 2.3 GHz Xeon processor. Our results demonstrate that our newly developed multiscale scanning method is capable of reliably detecting and locating MEQs in nearly real time during EGS stimulations.

ACKNOWLEDGMENTS

This material was based upon work supported by the U.S. Department of Energy, Office of Energy Efficiency and Renewable Energy (EERE), Office of Technology Development, Geothermal Technologies Office, under Award Number DE-AC52-06NA25396 to Los Alamos National Laboratory (LANL). The United States Government retains, and the publisher, by accepting the article for publication, acknowledges that the United States Government retains a non-exclusive, paid-up, irrevocable, world-wide license to publish or reproduce the published form of this manuscript, or allow others to do so, for United States Government purposes. This research used resources provided by the Los Alamos National Laboratory Institutional Computing Program, which is supported by the U.S. Department of Energy National Nuclear Security Administration under Contract No. 89233218CNA000001.

REFERENCES

Chen, Y., Huang, L., and EGS Collab Team "Microearthquake Hypocenter-Location and Focal-Mechanism Inversions for the EGS Collab Project: A Synthetic Study." Proceedings: 43rd Workshop on Geothermal Reservoir Engineering, Stanford University, Stanford, CA (2018a).

Chen, Y., Huang, L., Ajo-Franklin, J., Kneafsey, and EGS Collab Team "Toward Real-Time Microearthquake Event Detection and Location in Anisotropic Media Using a Multiscale Approach for EGS Collab Experiments." GRC Transactions, 42, (2018b), Dobson, P., Kneafsey, T.J., Blankenship, D., Valladao, C., Morris, J., Knox, H., Schwering, P., White, M., Doe, T., Roggenthen, W., Mattson, E., Podgorney, R., Johnson, T., Ajo-Franklin, J., and EGS Collab Team, "An Introduction to the EGS Collab SIGMA-V Project: Stimulation Investigations for Geothermal Modeling Analysis and Validation," GRC Transactions, 41, (2017), 837-849.

Gao, K., and Huang, L., "An improved rotated staggered-grid finite-difference method with fourth-order temporal accuracy for elastic-wave modeling in anisotropic media." Journal of Computational Physics, 350, (2017), 361-386.

Huang, L., Chen, Y., Gao, K., Fu, P., Morris, J., Ajo-Franklin, J., Nakagawa, S., and EGS Collab Team, "Numerical modeling of seismic and displacement-based monitoring for the EGS Collab Project." GRC Transaction, 41, (2017), 893-909.

Khadhraoui, B., Leslie, D., Drew, J., and Jones, R., "Real-time detection and localization of microseismic events", SEG Expanded Abstract, Denver, CO (2010).

Kneafsey, T.J., Dobson, P., Blankenship, D., Morris, J., Knox, H., Schwering, P., White, M., Doe, T., Roggenthen, W., Mattson, E., Podgorney, R., Johnson, T., Ajo-Franklin, J., Valladao, C., and the EGS Collab team "An Overview of the EGS Collab Project: Field Validation of Coupled Process Modeling of Fracturing and Fluid Flow at the Sanford Underground Research Facility, Lead, SD." Proceedings: 43rd Workshop on Geothermal Reservoir Engineering, Stanford University, Stanford, CA (2018).

Maxwell, S. "Microseismic Imaging of Hydraulic Fracturing." Society of Exploration Geophysicists (2014).

Nakata, N., and Beroza, G., "Reverse time migration for microseismic sources using the geometric mean as an imaging condition" Geophysics, 81, (2016), 251-259.

Schoenball, M., Ajo-Franklin, J., Blankenship, D., Cook, P., Dobson, P., Guglielmi, Y., Fu, P., Kneafsey, T., Knox, H., Petrov, P., Robertson, M., Schwering, P., Templeton, D., Ulrich, C., Wood, T., and EGS Collab Team "Microseismic monitoring of meso-scale stimulations for the DOE EGS Collab project at the Sanford Underground Research Facility." Proceedings: 44th Workshop on Geothermal Reservoir Engineering, Stanford University, Stanford, CA (2019).

Zhang, X., and Zhang, J., "Microseismic search engine for real-time estimation of source location and focal mechanism" Geophysics, 81, (2016), 169-181.